VIP DNA Damage

DOI: 10.1002/anie.200803235

Bond- and Energy-Selective Carbon Abstraction from D-Ribose by Hyperthermal Nitrogen Ions**

*Zongwu Deng, Ilko Bald, Eugen Illenberger, and Michael A. Huels**

The interaction of energetic, highly charged heavy particles with biological media bears significance in both heavy-ion cancer therapy[1] and space radiation risks for mission crews.[2,3] Heavy-ion traversal of living cells produces extremely high concentrations of secondary electrons, ions, and excited neutral species along the tracks, which can cause severe damage to the medium, including the nuclear DNA. The initial energetic secondary species are rapidly thermalized and solvated through multiple scattering energy-loss events, during and after which they interact with the DNA molecules, leading to cell death or mutations. Such genotoxic interactions have been extensively studied on the long time scales of thermally diffusion-limited chemical processes.[4] However, knowledge of the nascent (picosecond timescale) events immediately following primary ion irradiation, which link the initial physical processes and the later thermal diffusion-limited radiation chemistry, is still rudimentary, and it leads to major uncertainties in space radiation risk estimates to astronauts[3] and prohibits the development of global models for radiation damage.[5]

Early secondary electron damage to DNA occurs even at subionization electron energies by dissociative electron attachment (DEA), resulting in sugar–phosphate cleavage,[6,7] base loss,[8] single- and double-strand breaks,[9,10] and so forth, while hydrogen loss by DEA was found to be both bond- and site-selective.[11–14]

Regarding the formation of hyperthermal secondary species, heavy-particle radiation is distinct from conventional, sparsely ionizing photon or electron radiation in the sense that it imparts much higher kinetic energies to the secondary ion and neutral fragments. Recent measurements show that a primary heavy ion (MeV range) can produce secondary C^{n+}, O^{n+}, and N^{n+} ions ($n = 1$–3) from DNA bases with hyperthermal energies up to several 100 eV,[15,16] which is not observed for photon impact even at high energies. These hyperthermal ion fragments can cause further complex damage to DNA components in subsequent scattering events by collisional (physical) pathways at energies down to approximately 10 eV,[17] and reactive scattering (physicochemical) pathways at energies down to approximately 1 eV.[18] For example, the N^+ ion efficiently abstracts hydrogen atoms from DNA components at energies down to about 1 eV. Hydrogen abstraction is found to be bond- and charge-state-selective.[18] However, herein we show for the first time that the more severely damaging carbon abstraction from within the ring structure of D-ribose molecules by hyperthermal nitrogen ions exhibits a strong atom-site and energy selectivity, and we demonstrate that this selectivity is determined by the local chemical bond strengths.

Our experiments were conducted with a hyperthermal ion beam system.[17–19] It delivers a well focused, mass- and energy-selected, positive ion beam in the 1–100 eV energy range onto molecular films condensed on a polycrystalline platinum substrate in an ultrahigh-vacuum reaction chamber. Beams of approximately 30 nA Ar^+, 70 nA N^+ and N_2^+, focused at the target to a 2–4 mm spot, are used. The ion beams have an energy spread of approximately 1 eV full width at half maximum over the entire energy range. Multilayer molecular films are prepared by in vacuo evaporation and subsequent condensation onto atomically clean Pt substrates, which are cleaned by resistive heating to 1000 °C prior to each film deposition. Its cleanliness is verified by 200 eV Ar^+ secondary ion mass spectrometry (SIMS). The desorbing ionic reaction products during primary ion irradiation of molecular films are monitored by a quadrupole mass spectrometer (QMS, Hiden Analytical Ltd.) installed perpendicular to the ion-beam axis. The QMS measures desorbed ions with in vacuo energies of 0–5 eV. The sample surface is at approximately 60° with respect to the QMS axis during experiments.

D-ribose was purchased from Sigma Aldrich with purity of 99.5%, and D-[5-^{13}C]ribose was purchased from Cambridge Isotope Laboratories with isotopic purity of 98%. During experiments, the molecules were evaporated from a miniature oven at 60–70 °C and condensed on the substrate at room temperature. Film deposition rates were monitored with a quartz crystal microbalance and characterized in nanograms per square centimeter per minute. Film thickness is given by the known deposition rate and time. Since D-ribose films suffer some evaporative loss in high vacuum,[19] only thick films (ca. 1000 ng cm^{-2} or 20 monolayers) were used.

We find that both N^+ and N_2^+ ions efficiently abstract carbon atoms from D-ribose to form CN, which desorbs from the film as a CN^- ion. Figure 1a shows anion mass spectra between 23 and 28 amu produced by 50 eV Ar^+, N^+, and N_2^+ irradiation of D-ribose and D-[5-^{13}C]ribose films. Ar^+ irradi-

[*] Dr. Z. Deng, Dr. I. Bald,[+] Prof. Dr. E. Illenberger,[+] Prof. Dr. M. A. Huels
Ion Reaction Laboratory
Department of Nuclear Medicine and Radiobiology
Faculty of Medicine and Health Sciences, University of Sherbrooke
Sherbrooke, Quebec, J1H 5N4 (Canada)
Fax: (+1) 819-564-5442
E-mail: michael.huels@usherbrooke.ca

[+] Permanent address:
Institut für Chemie – Physikalische und Theoretische Chemie
Freie Universität Berlin, Takustrasse 3, 14195 Berlin (Germany)

[**] This work is supported by NSERC of Canada, and the Canadian Space Agency. A NATO grant allowed staff travel to Sherbrooke (I.B.).

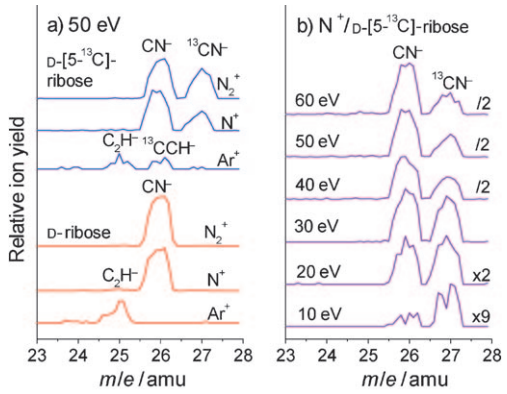

Figure 1. a) Anion mass spectra near 23–28 amu produced by 50 eV Ar^+, N^+, and N_2^+ irradiation of D-ribose (bottom) and D-[5-^{13}C]ribose (top) films. b) Mass spectra showing CN^- and $^{13}CN^-$ as a function of incident N^+ energy for D-[5-^{13}C]ribose films. The relative ion yields have been displaced vertically for ease of comparison.

ation produces C_2H^- anions at 25 amu, part of which appear as $^{13}CCH^-$ (26 amu) during irradiation of D-[5-^{13}C]ribose. No $C_2H_2^-$ is observed. Hence, the anion at 26 amu produced by N^+ and N_2^+ irradiation is unambiguously and exclusively assigned to CN^- as a result of carbon abstraction from D-ribose molecules. CN^- desorption strongly depends on the incident ion energy. Figure 2a shows the measured energy

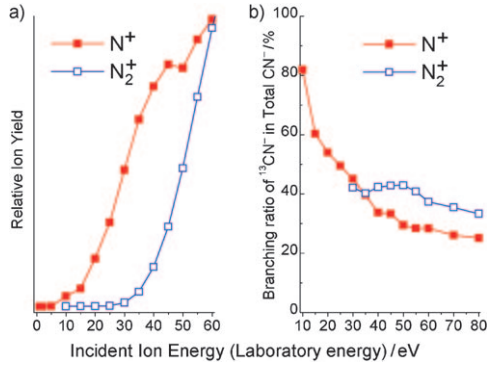

Figure 2. a) Incident energy dependence of CN^- desorption during N^+ and N_2^+ irradiation of D-ribose films. All CN^- ion yields are normalized in intensity at 60 eV for ease of comparison. b) Incident ion energy dependence of branching ratio of $^{13}CN^-$ yield in total CN^- desorption during N^+ and N_2^+ irradiation of D-[5-^{13}C]ribose films. The experimental uncertainty is about ±2 eV for the obtained threshold values and ±2.5% for the branching ratios. The ion's laboratory energy is the classical kinetic energy of the ion in the laboratory frame of reference.

dependence of CN^- desorption, yielding thresholds of approximately 5 and 30 eV for N^+ and N_2^+ impacts, respectively. The latter requires more energy to break the N_2^+ ion into atomic nitrogen, which then abstracts carbon to form CN. Collisional dissociation of N_2^+ is associated with neutralization upon impact in the films, which gives rise to two neutral nitrogen atoms. Hence, the reaction can proceed with both ionic and neutral atomic nitrogen, that is, the charge state of atomic nitrogen is not critical in carbon-atom abstraction. The reaction is rather driven by the formation of a strong C≡N triple bond (7.8 eV).[20] It should be noted that the CN^- anion must possess sufficient kinetic energy to overcome a charge-induced polarization barrier of about 1–1.5 eV at the surface of the film.[21] Thus, the present reactions will likely continue below the measured CN^- desorption threshold, yielding products with kinetic energies insufficient for desorption.

During N^+ and N_2^+ irradiation of D-[5-^{13}C]ribose, a significant amount of CN^- anion appears as $^{13}CN^-$ (27 amu, Figure 1a), suggesting specific abstraction of a carbon atom at C5. Figure 1b shows anion mass spectra between 23 and 28 amu as a function of incident N^+ energy between 10 and 60 eV. The results show that the relative intensity of $^{13}CN^-$ and CN^- signals strongly depends on incident ion energy. The branching ratio of $^{13}CN^-$ yield in total CN^- desorption is calculated by integrating the peak area and is shown in Figure 2b versus incident ion energy. It shows a significant increase from approximately 25 to 80% for N^+, and from about 33 to 43% for N_2^+, in both cases with decreasing energy from 80 down to 10 eV. Given a stoichiometric ratio of 20% for C5 in D-ribose, this indicates a selectivity for carbon abstraction at C5, particularly by N^+ ions, which depends inversely on the incident ion energy. Ion-impact-induced kinetic molecular fragmentation also exhibits site selectivity for C5, which is, however, ion-energy independent.[19] Here, the observed energy-dependent site-selectivity clearly demonstrates chemical effects on reaction selectivity. The reduced selectivity at higher ion energy is probably caused by the kinetic effect of ion impact, which overcomes the higher energetic barrier for carbon abstraction from other sites within the molecule; thus, at higher ion energies, kinetic effects leading to carbon abstraction dominate and lead to stoichiometric distribution of CN^- products.

For a surface-atom abstraction reaction, in which a gas-phase reagent approaches and abstracts an atom from the surface to form a product which then desorbs from the surface, the probability of the reaction will be determined by the strength of the bonds to be formed (the reactivity between the approaching reagent and the surface atom), the strength of the bonds to be cleaved on the surface, and the accessibility of the surface atom to the approaching reagent (the steric effects). In this case, the formation of CN^- by carbon abstraction from D-ribose by N^+/N_2^+ ions is a result of multiple chemical bond cleavage, chemical bond formation, ionization of CN, and its subsequent desorption from the film. Because the chemical bond formation, ionization, and desorption of CN are expected to be site-independent, and because we anticipate no significant steric effect in favor of C5, the observed high selectivity for CN^- formation from C5 implies a weaker bond at C5 than at the other carbon atoms. To discuss this site selectivity, we must examine the molecular structure of D-ribose in films. D-ribose can adopt different conformations depending on the medium.[22–25] In RNA, D-ribose appears in its furanose form (a five-membered ring), whereas the molecule tends to adopt its pyranose form (a six-membered ring) in both condensed and gas phases (Figure 3).[22] This suggests that the present results are from hyperthermal nitrogen ion interaction with the pyranose form of D-ribose.

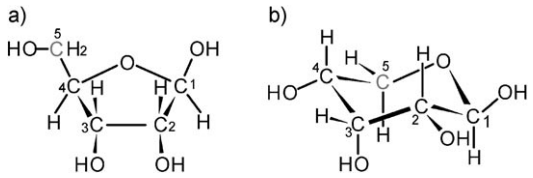

Figure 3. The furanose (a) and pyranose (b) structures of D-ribose. Note the location of C5 as well as the presence (absence) of a hydroxy group on C5 in the furanose (pyranose) form.

The C5 atom is converted from an exocyclic position in the furanose form to an endocyclic position in the pyranose form. The weak local chemical bonds at C5 can be partly accounted for first by the weak endocyclic C–O bonds (in this case, both the C5–O and C1–O bonds) with respect to the endocyclic C–C bonds.[26–28] This difference is demonstrated by the fact that the cleavage of the endocyclic C–O bond is always the major primary process during photolysis of cyclic ethers.[26] The formation of intramolecular hydrogen bonds to yield an energetically favorable D-ribose conformation in the condensed phase further decreases the local bond strength at C5 with respect to C1, as addressed below.

Conformations of D-ribose and monosaccharides have been extensively studied.[22–25] In a given medium, a specific conformation depends on its potential (internal) energy and temperature. The relative potential energy of a conformation is given by several factors. In the gas phase, these include (in order of significance): intramolecular hydrogen bonding $\gg$ anomeric effect $>$ steric effect $\gg \Delta 2$ effect.[23] Intramolecular hydrogen bonding is the dominant and stabilizing factor and can significantly reduce the potential energy of a conformation. In solution, the solvent also plays a role through solute polarization and solvent–solute hydrogen bonding.[23] In the condensed phase, intermolecular hydrogen bonding may exist. Interplay of these factors determines the total potential energy of the conformers and their final composition in a given medium.[22,23] While the strength of a single H-bond in the furanose form sometimes appears higher than in the pyranose form, it is usually counteracted by the smaller number of H-bonds, the stronger unfavorable effect of steric repulsion, and dipole interactions.[22] Thus, the pyranose form always has lower potential energy and dominates in both gas and condensed phases and in most solutions.[22–25]

Experimental results suggest that D-ribose adopts the pyranose form in both condensed and gas phases and maintains this structure throughout evaporation.[22] Computational results suggest that in the pyranose form D-ribose can develop three intramolecular hydrogen bonds among the OH groups of C2, C3, and C4 to form the energetically lowest state at 0 K.[22] A second-lowest state (ca. 0.3 kcal mol^{-1} higher in potential energy) is formed by intramolecular hydrogen bonding among the OH groups of C1, C2, C3, and C4.[22] This likely increases the local bond strength for the relevant carbon atoms with respect to C5. The latter is not involved in any intramolecular hydrogen bonding, as it bears no OH group (Figure 3b). Meanwhile, to maximize the effect of hydrogen bonding, the favorable conformation will optimize the molecular geometry, that is, the relevant bond angles and lengths.[22] This will introduce unfavorable steric repulsion and dipole interactions and thus weaken the bond strength of the ring atoms (increase the internal energy). The optimized molecular geometry is thus a compromise between these two effects, and the local bond strength of the atoms involved in intramolecular H-bonding (C1, C2, C3, and C4) is compensated by H-bond formation, whereas that of C5 is not. The net result is a maximum decrease in potential energy of the whole conformation.

The fluctuation of local internal energy in these processes can be estimated semiquantitatively according to computational results. The potential energy difference between the first two lowest states of D-ribose in the furanose form is calculated to be approximately 2.3 kcal mol^{-1} at 0 K,[22] owing to an additional hydrogen bond in the lowest state, and can be taken as the average intramolecular hydrogen bond strength in D-ribose. This value is reasonable compared to hydrogen bond strengths of approximately 4.58 kcal mol^{-1} in water dimers.[24] The difference in hydrogen bond strength between D-ribose and water dimers can be ascribed to two factors: 1) D-ribose provides a less favorable hydrogen bonding geometry than water dimers, which decreases the strength of the formed hydrogen bond. 2) To form intramolecular hydrogen bonds, bond angles and lengths in D-ribose have to be adjusted, which introduces additional internal energy and thus counteracts the advantage of hydrogen bonding. We assume that half of the difference (ca. 1.1 kcal mol^{-1}) can be attributed to each of the two factors (this is likely overestimated). As a result, formation of three hydrogen bonds in D-ribose in the energetically lowest pyranose state can introduce a net decrease of approximately 6.9 kcal mol^{-1} in potential energy, which contributes to local chemical bond strength among the relevant atoms. It also leads to about 3.3 kcal mol^{-1} in internal energy, which we assume is evenly distributed in the ring atoms and the OH groups involved in the hydrogen bond formation. On average, approximately 0.4 kcal mol^{-1} may go to C5. More internal energy is introduced to the furanose form owing to stronger steric repulsion and dipole interactions, which results in the lowest furanose state being located about 2 kcal mol^{-1} above the lowest pyranose state.[22] Consequently, the pyranose form dominates the molecular structure of D-ribose in both the gas phase and the condensed phase, and moreover, C5 appears to be the weakest point in the pyranose ring of D-ribose. This may be the cause of the observed site-selectivity for C5 in both carbon abstraction from genetic sugars as well as in their kinetic-impact molecular fragmentation.[19]

While the observed site selectivity for carbon abstraction from the pyranose form of D-ribose cannot be applied directly to cells, the correlation between reaction-site selectivity and local chemical bond strength nonetheless has important biological implications. In RNA or DNA the chemical bond strength in bases is strongly enhanced relative to sugar moieties by conjugation among ring atoms. The sugar units experience strong ring strain in the furanose form without the stabilizing effects of intramolecular H-bonds. Thus, in DNA/RNA, local chemical bond strength of ring atoms in sugars is expected to be much weaker than in bases, and our present results imply that the sugar moiety will be more vulnerable

than the bases during reactive scattering of secondary atomic nitrogen ions produced with hyperthermal energies by heavy-ion tracks.[15,16] Abstraction of C3, C4, or C5 from sugars leads to a single-strand break, and abstraction of C1 leads to base loss (see to Figure 3a). Abstraction of C1, C2, C3, or C4 is associated with destruction of the ring structure. As observed here, at very low secondary-ion energies, in genetic sugars abstraction of C1 or C4 will dominate owing to the weak endocyclic C–O bond in the furanose form.

In conclusion, reactive scattering of hyperthermal nitrogen ions from D-ribose films leads to efficient carbon abstraction to form CN products. The reaction exhibits a strong site and energy selectivity for the C5 atom of D-ribose in its pyranose form, owing to the local chemical bond strength at C5. We suggest that the RNA/DNA sugar backbone will also be vulnerable to such site-selective damage by the reactive hyperthermal secondary ions produced along heavy-ion tracks in cells.

Received: July 3, 2008
Published online: October 27, 2008

Keywords: atom abstraction · bioorganic chemistry · DNA · ion scattering · mass spectrometry

[1] D. Schulz-Ertner, A. Nikoghosyan, C. Thilmann, T. Haberer, O. Jäkel, C. Karger, G. Kraft, M. Wannenmacher, J. Debus, *Int. J. Radiat. Oncol. Biol. Phys.* **2004**, *58*, 631.
[2] E. R. Benton, E. V. Benton, *Nucl. Instrum. Methods Phys. Res. Sect. B* **2001**, *184*, 255.
[3] Strategic Program Plan for Space Radiation Health Research. NASA, Washington DC, **1998**.
[4] C. von Sonntag, *The Chemical Basis for Radiation Biology*, Taylor and Francis, London, **1987**.
[5] Research Needs and Opportunities in Radiation Chemistry Workshop, DOE Final Report SC-0003, US Department of Energy, **1998**.
[6] Y. Zheng, P. Cloutier, D. J. Hunting, L. Sanche, J. R. Wagner, *J. Am. Chem. Soc.* **2005**, *127*, 16592.
[7] C. König, J. Kopyra, I. Bald, E. Illenberger, *Phys. Rev. Lett.* **2006**, *97*, 018105.
[8] Y. Zheng, P. Cloutier, D. J. Hunting, J. R. Wagner, L. Sanche, *J. Am. Chem. Soc.* **2004**, *126*, 1002.
[9] B. Boudaïffa, P. Cloutier, D. Hunting, M. A. Huels, L. Sanche, *Science* **2000**, *287*, 1658.
[10] M. A. Huels, B. Boudaïffa, P. Cloutier, D. Hunting, L. Sanche, *J. Am. Chem. Soc.* **2003**, *125*, 4467.
[11] H. Abdoul-Carime, S. Gohlke, E. Illenberger, *Phys. Rev. Lett.* **2004**, *92*, 168103.
[12] S. Ptasińska, S. Denifl, V. Grill, T. D. Märk, E. Illenberger, P. Scheier, *Phys. Rev. Lett.* **2005**, *95*, 093201.
[13] S. Ptasińska, S. Denifl, V. Grill, T. D. Märk, P. Scheier, S. Gohlke, M. A. Huels, E. Illenberger, *Angew. Chem.* **2005**, *117*, 1673; *Angew. Chem. Int. Ed.* **2005**, *44*, 1647.
[14] S. Ptasińska, S. Denifl, P. Scheier, E. Illenberger, T. D. Märk, *Angew. Chem.* **2005**, *117*, 7101; *Angew. Chem. Int. Ed.* **2005**, *44*, 6941.
[15] J. de Vries, R. Hoekstra, R. Morgenstern, T. Schlathölter, *Phys. Rev. Lett.* **2003**, *91*, 053401.
[16] T. Schlathölter, R. Hoekstra, S. Zamith, Y. Ni, H. G. Muller, M. J. J. Vrakking, *Phys. Rev. Lett.* **2005**, *94*, 233001.
[17] Z.-W. Deng, I. Bald, E. Illenberger, M. A. Huels, *Phys. Rev. Lett.* **2005**, *95*, 153201.
[18] Z.-W. Deng, I. Bald, E. Illenberger, M. A. Huels, *Phys. Rev. Lett.* **2006**, *96*, 243203.
[19] I. Bald, Z.-W. Deng, E. Illenberger, M. A. Huels, *Phys. Chem. Chem. Phys.* **2006**, *8*, 1215.
[20] Z.-W. Deng, R. Souda, *J. Chem. Phys.* **2002**, *117*, 6235.
[21] P. Rowntree, L. Parenteau, L. Sanche, *J. Phys. Chem.* **1991**, *95*, 4902; P. Rowntree, L. Parenteau, L. Sanche, *J. Phys. Chem.* **1991**, *95*, 523.
[22] L. P. Guler, Y.-Q. Yu, K. I. Kenttämaa, *J. Phys. Chem. B* **2002**, *106*, 6754.
[23] B. Ma, H. F. Schaefer III, N. L. Allinger, *J. Am. Chem. Soc.* **1998**, *120*, 3411.
[24] J.-H. Lii, B. Ma, N. L. Allinger, *J. Comput. Chem.* **1999**, *20*, 1593.
[25] W. Pigman, D. Horton, *The Carbohydrates: Chemistry and Biochemistry*, Academic Press, New York, **1972**.
[26] A. A. Scala, E. W.-G. Diau, Z. H. Kim, A. H. Zewail, *J. Chem. Phys.* **1998**, *108*, 7933.
[27] Z. Diaz, R. D. Doepker, *J. Phys. Chem.* **1978**, *82*, 10.
[28] A. A. Scala, W. J. Rourke, *J. Photochem.* **1987**, *37*, 281.

